XX Polish Fluid Mechanics Conference,
Gliwice, 17-20 September 2012

NUMERICAL STUDY OF THE FLOW STRUCTURE AND HEAT TRANSFER ON A ROTATING DISK SURFACE UNDER ANNULAR JET IMPINGEMENT

Kamil KIEŁCZEWSKI[1], Ewa TULISZKA-SZNITKO[1]
[1]*Institute of Thermal Engineering, Poznań University of Technology, Poland*
E-mail: kamil.k.kielczewski@gmail.com; ewa.tuliszka-sznitko@put.poznan.pl

Abstract

In the paper we analyze numerical effectiveness of the new parallelized version of the DNS/LES code (Tuliszka et al. 2009a,b) prepared to study the 3D flow with heat transfer in rotor/stator and rotor/rotor cavity. Parallelization allows us to perform computations on a mesh up to 60 million colocation points. Two flow cases are considered: the axial annular jet flow impinging on a rotating disk and flow with heat transfer in rotor/stator configuration of aspect ratio L=45. Both flow cases are of interest as simple flows with heat transfer, very suitable for investigating the transitional and turbulent boundary layer physics. These flow cases can also be used as benchmarks for modeling more complex flows with heat transfer which are applicable in the designing of rotating machinery.

Key words: DNS/LES, parallelization, jet flow, rotating flow, turbulence, heat transfer

INTRODUCTION

Turbulence and laminar-turbulent transition in fluid still belong to the most difficult problems in physics. The large diversity of phenomena associated with turbulence makes this branch of physics challenging and intriguing. Most of our knowledge comes from the DNS/LES or experimental measurements. Usually the objective of DNS and LES of strongly 3D flows is to explore turbulence characteristics and physical mechanism of laminar boundary layer transition, and also to create reference data to assess the validity of under-resolved approximations. In spite of large progress on this important topic many challenges remain. In the paper we investigate two strongly 3D flow cases: The first is the flow between two rotating disks with the superimposed axial inflow and radial outflow (this flow case can be considered as confine annular jet impinging on the rotating disk). In the second case we investigate the flow with heat transfer in rotor/stator cavity of large aspect ratio L=45 (this flow case is dominated by viscous forces). Both flows exhibit strong skewing of the velocity vector across the boundary layers which is typical for the 3D boundary layer and are very suitable for investigating transitional and turbulent boundary layer phenomena.

Flows in rotating disks system are not only a subject of fundamental interest as prototype flows with three dimensional boundary layers but are also a topic of practical importance (typical configurations are cavities between rotating compressors and turbines' disks). The flows with jets are of great importance in many engineering problems, such as the cooling, heating and drying processes. The axial through flow (rotor/stator configuration) with heat transfer was numerically investigated by Poncet and Schiestel (2007) using RANS method. Cylindrical jet flow impinging on the heated rotating disk was investigated numerically and experimentally by Minagawa, Obi (2004), Astarita, Cardone (2008), Chen, Lee, Wu (1998), Lallave, Rahman, Kumar (2007). The evolution of jets is strongly affected by the inlet condition (condition at the nozzle exit) and outlet condition. The inlet condition was

differently formulated by different authors. Fröhlich and Rodi (2002) used mean flow with imposed random perturbations. Hadziabdic and Hanjalic (2008) generated the inflow condition by a separate LES simulation of the fully developed turbulent pipe flow. They stored the velocity field obtained in the exit of the pipe at every time step and then used it to define the inlet condition for jet computations. Tsubokura et al. (2003) assumed mean dimensionless velocity profile $W(r)/W_0=[1-(2r/D)^8]$ and superimposed on it the non-stationary disturbances. Tsubokura et al. (1997) and Le Song, Prud'homme (2007) used the empirical formula for velocity profile at the nozzle, $W(r)/W_0=[1-(2r/D)^{10}]$. As for the outlet condition, most authors use the convective condition - Hadziabdic and Hanjalic (2008) defined this condition by the hyperbolic convective equation:

$$\frac{\partial u}{\partial t} + u_c \frac{\partial u}{\partial r} = 0 \tag{1a}$$

where u_c is the mean convective velocity and u is the radial component of the velocity vector. Convective velocity is estimated from the balance of mass:

$$\int_{S_{inlet}} w ds = \int_{S_{outlet}} u_c ds \tag{1b}$$

where w is the axial velocity component.

In the rotor/stator configuration two main scenarios of laminar-turbulent transition have been identified (Schouveiler et al., 2001). The first scenario is typical for configurations of aspect ratio L = 2 – 35 and is characterized by a sequence of supercritical bifurcations. The flow is dominated by Coriolis and centrifugal forces. It is the so called Batchelor flow which consists of two boundary layers separated by the inviscid rotating core. In Batchelor flows the non-isothermal conditions were also taken into consideration (Randriamampianina et al. 1987; Poncet, Schiestel, 2007; Tuliszka-Sznitko et al. 2009a, b, 2012; Pellé, Harmand, 2007). In the second scenario, typical for large aspect ratio ($L \geq 45$), formation of localized turbulent structures typical for subcritical transition are observed. When L is sufficiently large, the flow is similar to torsional Couette flow (pure shear flow with joined boundary layers). Schouveiler et al. (2001) showed that in such a flow case the first bifurcation leads to a network of spiral vortices. For higher Reynolds numbers turbulent spots SP and solitary waves SW appear.

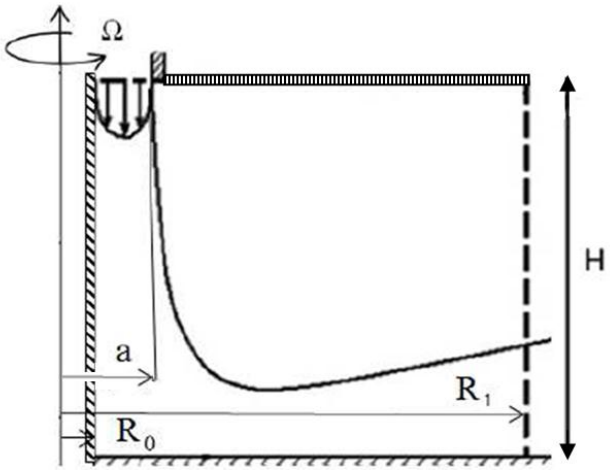

a)

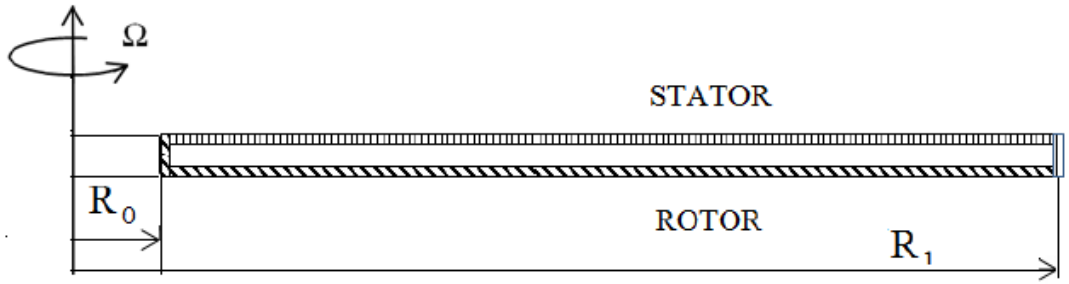

b)

Figure 1. Schematic pictures of numerical domains; a) the flow case with axial jet, b) rotor/stator cavity

The purpose of the present paper is to check effectiveness of the new parallelized version of the code described in Tuliszka-Sznitko et al. (2009a, b, 2012). This new version allows us to perform computations using up to 60 million collocation points. In consecutive sections we present: the mathematical and numerical models (including boundary conditions for jet flow cases) and preliminary results obtained for considered flow cases.

MATHEMATICAL MODEL AND NUMERICAL APPOACH

The geometrical domain is presented in Figure 1a and b. The upper and the bottom disks can rotate at a uniform angular velocity around the central axis (we consider rotor/rotor and rotor/stator configuration). The half of interdisk spacing is depicted by h (H=2h, Figure 1). The flow is controlled by the following physical parameters: the Reynolds number, based on the external radius of the disks R_1 and on the angular velocities of the rotor $\mathrm{Re} = \Omega R_1^2 / \nu$, the aspect ratio $L=(R_1 - R_0)/2h$, the curvature parameter $\mathrm{Rm} = (R_1 + R_0)/(R_1 - R_0)$, the Prandtl number Pr=0.71 and the thermal Rossby number $B=\beta(T_2 - T_1)$ (where β is the thermal expansion coefficient, T_1 and T_2 are temperature of the chosen walls). For the flow with the axial jet additional geometrical parameter $a_1 = (a - R_0)/(R_1 - R_0)$ is introduced which characterizes the inlet of the flow.

The dimensionless components of the velocity vector in radial, azimuthal and axial directions are denoted by $u = U/\Omega R_1$, $v = V/\Omega R_1$, $w = W/\Omega R_1$. The dimensionless axial and radial coordinates are: $z = Z/h$, $z \in [-1, 1]$, $r = (2R - (R_1 + R_0))/(R_1 - R_0)$, $r \in [-1, 1]$. The dimensionless temperature is defined in the following manner: $\Theta = (T - T_1)/(T_2 - T_1)$.

The numerical solution is based on a pseudo-spectral Chebyshev-Fourier-Galerkin approximation. The Gauss-Lobatto collocation points in radial and axial directions are used: $r_i = \cos(\pi i / N)$ for $0 \le i \le N$ and $z_i = \cos(\pi i / M)$ for $0 \le i \le M$ to ensure high accuracy of the solution inside the very narrow boundary layers at the disks. The uniform mesh is used in azimuthal direction; $\varphi_k = 2\pi k/K$, k=0, 1, 2…K-1. The time scheme is semi-implicit and second-order accurate - it corresponds to a combination of the second-order backward differentiation formula for the viscous diffusion term and the Adams-Bashforth scheme for the non-linear terms. The incorporated dimensionless time step is δt =0.001-0.00001. The method uses a projection scheme to maintain the incompressibility constraint; Tuliszka-Sznitko, Zieliński, Majchrowski (2009a and b).

The initial condition corresponds to a fluid at the rest. The boundary conditions for the rotor/stator flow are as follows: The outer cylinder of radius R_1 and inner cylinder of radius

R_0 are attached to the stator and rotor, respectively. The no-slip boundary conditions are used with respect to all rigid walls u=w=0. For the azimuthal velocity component, the boundary conditions are v=0 on the rotating disk, and $v = -(Rm + r)/(Rm + 1)$ on the stator. However, in order to eliminate the singularity of the azimuthal velocity component at the junction between the stationary outer cylinder and rotor, and between rotating inner cylinder and stator, the azimuthal velocity component are regularized by exponential profiles (Tavener et al., 1991; Randriamampianina et al., 1997, 2001). The thermal boundary conditions are as follows:

$\Theta = 1$ for z= -1.0, $-1.0 \le r \le 1.0$ and for outer cylinder (2a)

$\Theta = 0$ for z =1.0, $-1.0 \le r \le 1.0$ and for inner cylinder (2b)

For flow cases with the axial jet the nozzle flow is treated by prescribing an assumed velocity profile (we assumed constant value). In the outer cylinder we assumed constant radial velocity component (in rotor/stator configuration) and we applied convective condition in rotor/rotor configuration. Convective condition in the outer cylinder was implemented as follows:

$$u^{n+1} = \frac{1}{3}\left\{4u^{n} - u^{n-1} - 2\,\delta t\, u_c\left(2\left(\frac{\partial u}{\partial r}\right)^{n} - \left(\frac{\partial u}{\partial r}\right)^{n-1}\right)\right\} \tag{3}$$

where δt is the increment of time, n+1, n and n-1 indicate consecutive time sections.

Numerical investigations of both flow cases require a refined meshes with large number of colocation points. To meet this requirement we applied OpenMP technology to code described in Tuliszka-Sznitko, Zieliński, Majchrowski (2009a and b). Parallelization of the DNS code has been done on the cluster Reef in Poznań Supercomputing and Networking Center (we used Intel MKL). Preliminary computations performed in the frame of this paper allowed us to estimate CPU time needed per one iteration: for the mesh $100\times100\times100$ we need 0.8 second per iteration; for $400\times150\times400$ about 29 seconds (8-cores, 2.3 GHz).

SELECTED RESULTS

Verification of the parallelized version of the code

Parallelized version of the DNS code was verified by comparison of obtained results with those published previously in Tuliszka-Sznitko et al. (2012). Comparative calculations were performed for the following configurations: L=5, 25, 35, Rm=1.8, B=0.1 and for different Reynolds numbers. Figures 2a and b present comparison of the axial profiles (L=25, Re=180000) of the radial and azimuthal velocity components obtained by LES (NPR=280, NPZ=131, NPA=260, Tuliszka-Sznitko et al. 2012) with the present DNS results $(440\times171\times440)$. We can see that differences are negligible small.

Figures 3a and b show comparison of the Reynolds stress tensor components $\overline{u'u'}^{0,5}$, $\overline{v'v'}^{0,5}$, $\overline{w'w'}^{0,5}$ and the turbulent heat flux tensor components $\overline{(\Theta'u')}$, $\overline{(\Theta'v')}$, $\overline{(\Theta'w')}$ obtained using LES code and parallelized DNS code. We observe that magnitudes of the azimuthal Reynolds stress tensor component $\overline{v'v'}^{0,5}$ and $\overline{(\Theta'v')}$ in the central core of cavity obtained in the present paper are slightly smaller than these published previously in Tuliszka-Sznitko et al. (2012).

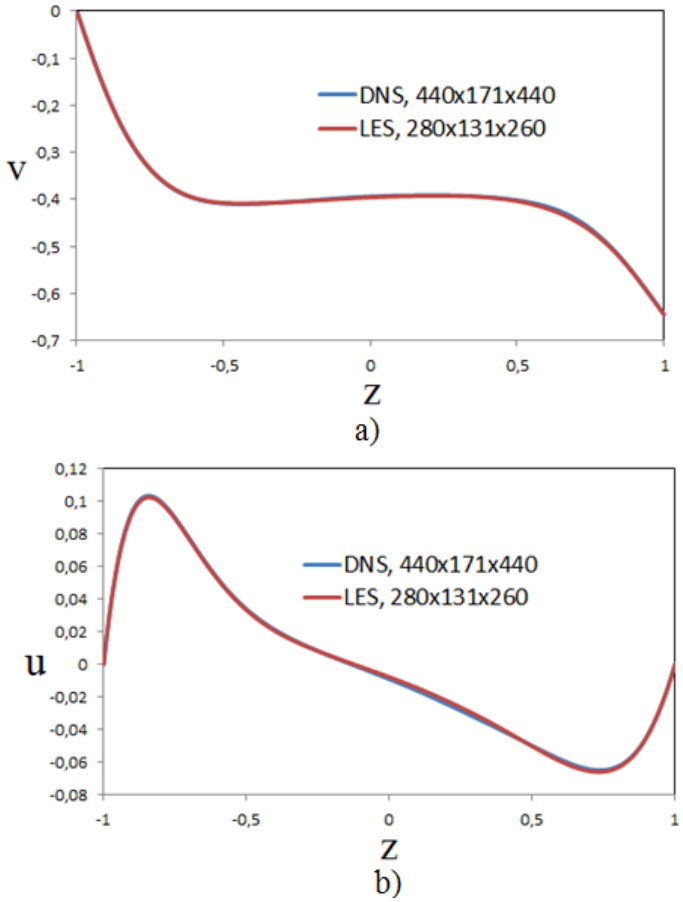

Figure 2. The axial profiles of the radial (a) and azimuthal (b) velocity components obtained in present paper (parallelized DNS code) for L=25, Re=180000, B=0.1, Rm=1.8 and published in Tuliszka-Sznitko et al. (2012). Middle section of cavity

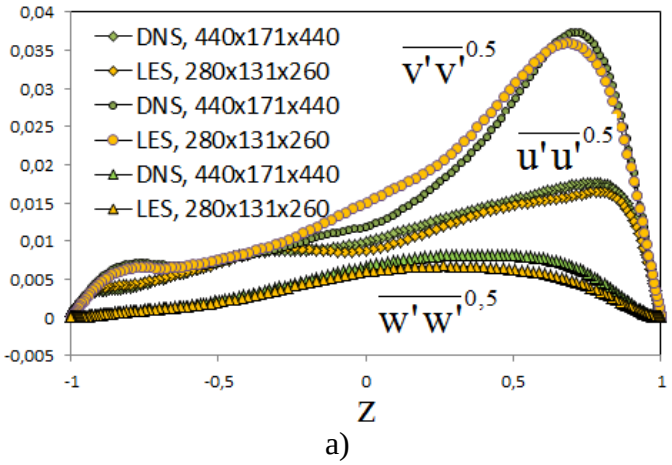

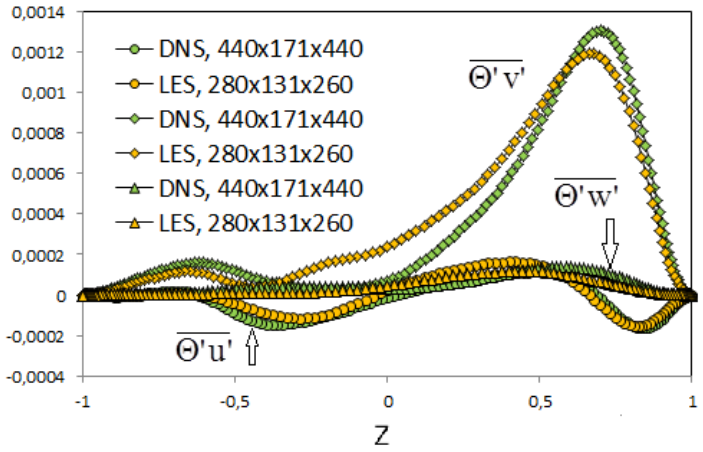

b)

Figure 3. a)The normal Reynolds stress tensor components $\overline{u'u'}^{1/2}$, $\overline{v'v'}^{1/2}$, $\overline{w'w'}^{1/2}$ versus z. b) turbulent heat flux components $(\overline{\Theta'u'})$, $(\overline{\Theta'v'})$, $(\overline{\Theta'w'})$ versus z. Comparison of the results obtained in the present paper (by parallelized DNS code) and results published in Tuliszka-Sznitko et al. (2012). L=25, Rm=1.8, Re=180000. Middle section of cavity

To show the accuracy of the mathematical description of the flow near the disks we analyzed wall coordinate $(\Delta z^+)_{min}$ in terms of r, where $(\Delta z^+)_{min}$ is based on the smallest cell in the axial direction; $(\Delta z^+)_{min} = z_{min}[Re/L(Rm+1)]^{1/2}[(\partial u/\partial z)_w^2 + (\partial v/\partial z)_w^2]^{1/4}$. The results presented in Figure 4 were obtained for the aspect ratio L=25, Reynolds numbers Re=180000 and on two meshes: NPR=440, NPZ=171, NPA=440 (by parallelized DNS code) and NPR=280, NPZ=131, NPA=260 (by LES code). For both flow cases $(\Delta z^+)_{min}$ is far smaller than 1.0 which guarantees a precise description in the near-wall areas (Séverac et al. 2007).

The exemplary iso-surfaces of the axial velocity component (w=0.004) obtained for Re=230000, L=25, Rm=1.8 are presented in Figure 5 (ParaView editor).

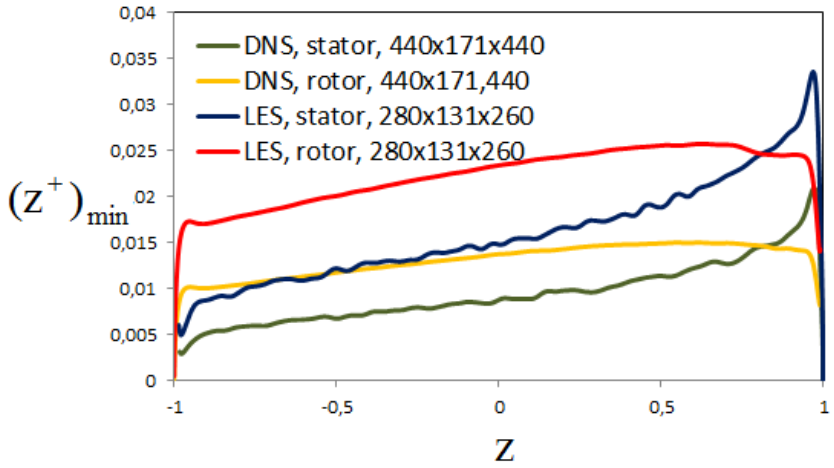

Figure 4. Distribution of $(\Delta z^+)_{min}$ in terms of r. Re=180000, L=25, Rm=1.8, B=0.1

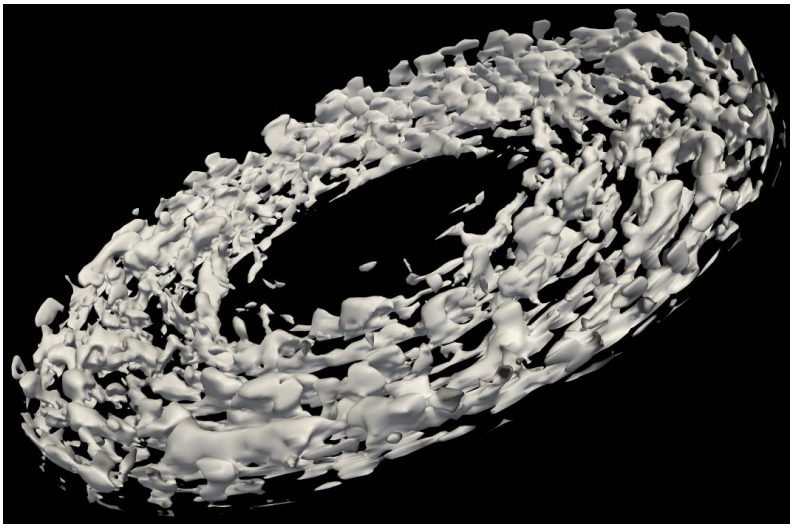

Figure 5. The iso-surface of the axial velocity component (w=0.004) obtained for Re=230000, L=25, Rm=1.8. Present paper results

Preliminary results obtained for axial annular jet flow

In the present paper some preliminary computations have been performed for the flow with axial annular jet impinging on the rotating disk (Figure 1). Two flow cases were tested: axial jet in rotor/stator cavity (Figure 6) and in rotor/rotor cavity (Figures 7a and b). Figure 6 presents the meridian flow obtained for the axial velocity component at the entrance of cavity equal Cw=0.29, Re=10000, L=6, Rm=1.8, $a_1 = 0.0216$ (rotor/stator configuration, NPR=150, NPZ=150, NPA=150). In Figure 6 only sources area is visible. In this flow case air is introduced into the cavity through the stator (top disk) near the inner cylinder and is extracted through the outer cylinder. We assume uniform inlet and outlet. From Figure 6 we can see that fluid enters the cavity through top disk and axial jet impinges on the bottom rotating disk. In the source area large vortex is observed which intensive redistribution of the fluid in this area. Then fluid is pumped radially outward along rotor as a wall jet. Near the outer cylinder flow is redistributed again.

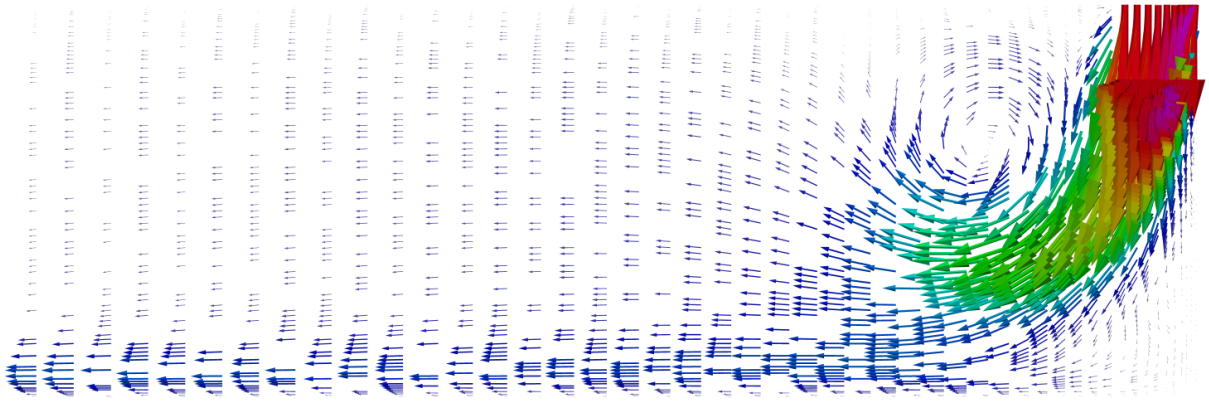

Figure 6. Meridian flow near the source area. The axial velocity component at the entrance Cw=0.29, Re=10000, L=6, Rm=1.8, $a_1 = 0.0216$ (rotor/stator configuration, $150 \times 150 \times 150$).

Figure 7a presents meridian flow in the rotor/rotor configuration with axial annular jet ($a_1 = 0.013955$, Cw=0.14, Re=10000, L=15, Rm=1.8). Computations were performed on 8 million collocation points $(200 \times 200 \times 200)$. In this flow case convective boundary condition

was applied at the outer cylinder (equation 3). From Figure 7a we can see that fluid is introduced into the cavity axially through the top disk near the inner cylinder (source area) and then is pumped radially outward as a wall jets along both rotating disks (Ekman layers). Similar computations were performed in paper Tuliszka-Sznitko, Zieliński (2008) for higher Re which causes more intensive redistribution of the fluid in the source area.

Preliminary computations performed on the axial jet flows gave us the opportunity to test methods of implementing the convective condition on the outer cylinder as well as opportunity to estimate the CPU time and number of collocation points needed for such investigation. We can conclude that the parallelized DNS cod presented in this paper is well-prepared numerical tool to study the flow with axial and wall jets.

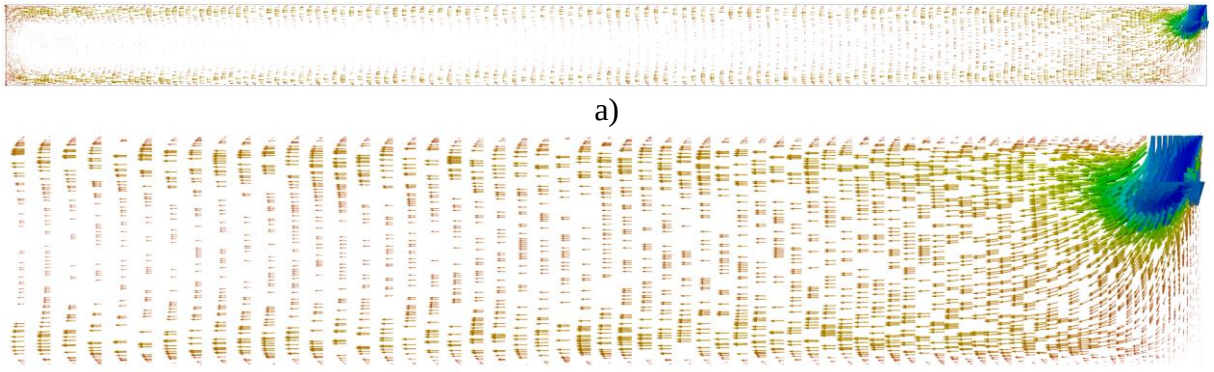

a)

b)

Figure 7. Meridian flow in rotor/rotor cavity with axial annular jet. a) whole cavity, b) source area. The axial velocity component at the entrance Cw= 0.14, Re=10000, L=15, Rm=1.8, $a_1 = 0.013955$, (rotor/rotor configuration, $200 \times 200 \times 200$).

Computations performed for rotor/stator cavity of L=45

In the paper we also investigated the flow with heat transfer in rotor/stator cavity of aspect ratio L=45, Rm=1.8, B=0.1 (NPR=300, NPZ=171, NPA=360). In the frame of boundary conditions described in equations 2, flow is pumped along the heated rotor (bottom disk) towards the outer cylinder, then is lifted up along the heated stationary outer cylinder. Flow recirculates along the cooled stator, and finally is going down along the cooled rotating inner cylinder. The axial profiles of the azimuthal velocity component obtained in three sections r=0.8139, 0, -0,8139 and for Re=320000 are presented in Figure 8. We can see from Figure 8 that Batchelor flow exists only in the section r=0.8139; that means that the flow consists of two boundary layers on each disk, separated by an inviscid rotating core in which the velocity gradient is weak. The turbulence is concentrated in the stator with a maximum at the junction between the stator and outer cylinder (Figure 9 presents the Reynolds stress tensor components obtained for Re=320000). Further increase of the Reynolds number (above 320000) for this flow case requires the use of modeling (we plan to use spectral vanishing viscosity method). Simultaneously we started computations of the flow with heat transfer in rotor/stator cavity of the aspect ratio L=65. We believed that developed numerical tools will allow us to investigate this fully dominated by viscous forces flow case.

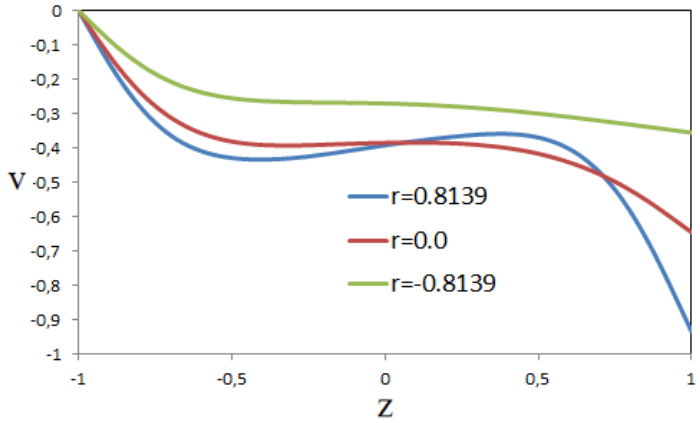

Figure 8. The axial profiles of azimuthal velocity component obtained in different sections of cavity. Re=320000, L=45, Rm=1.8, B=0

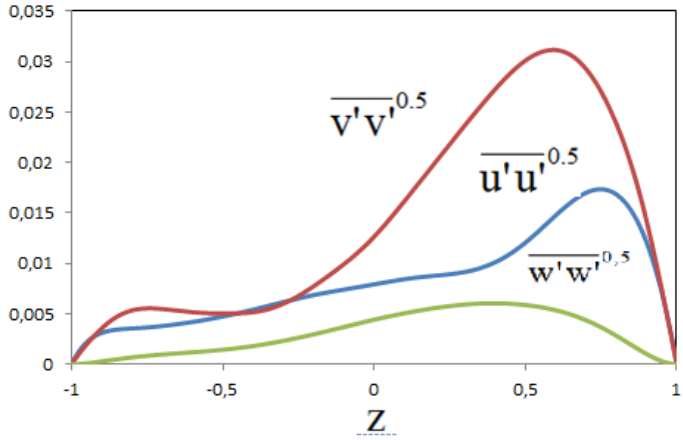

Figure 9. The Reynolds stress tensor components obtained in the middle section of cavity. Re=320000, L=45, Rm=1.8, B=0

CONCLUSIONS

In the paper the preliminary results obtained by using the new parallelized version of the code described in Tuliszka-Sznitko et al. (2009a, b) have been presented. Computations are focused on two strongly 3D flow cases: the axial jet flow and the flow in rotor/stator cavity of aspect ratio L=45 and curvature parameter Rm=1.8. The new parallelized (by OpenMP technology) version of the code allows us to perform computations on up to 60 million colocation points (further increase requires MPI technology). DNS computations (rotor/stator cavity, L=45) have been performed for Reynolds number up to Re=320000; for higher Re it is necessary to used LES method (we plan to incorporate spectral vanishing viscosity method - SVV method). Additionally, for the axial jet flow the multi-domain method will be used.

ACKNOWLEDGEMENTS

The computations were carried out in the Poznan Supercomputing and Networking Center, which is gratefully acknowledged.

REFERENCES

Astarita T., Cardone G., (2008): *Convective heat transfer on a rotating disk with a centred impinging round jet*, Int. Journal of Heat and Mass Transfer, Vol. 51, pp. 1562–1572

Chen Y.-M., Lee W.-T., Wu S.-J., (1998),: *Heat (mass) transfer between an impinging jet and a rotating disk,* Int. Journal of Heat and Mass Transfer, Vol. 34, pp. 195-201

Fröhlich J., Rodi W., (2002): *Introduction to large eddy simulation of turbulent flows, In Closure Strategies for Turbulent and Transitional Flows*, Ed. B. Launder, N.D. Sandham, pp. 267-298, Cambridge University Press

Hadziabdic M., Hanjalic K., (2008): *Vortical structures and heat transfer in a round impinging jet,* J. Fluid Mech., Vol. 596, pp. 221-260

Lallave J. C., Rahman M. M., Kumar A., (2007): *Numerical analysis of heat transfer on a rotating disk surface under confined liquid jet impingement,* Int. Journal of Heat and Fluid Flow, Vol. 28, pp. 720–734

Le Song G., Prud'homme M., (2007): *Prediction of coherent vortices in an impinging jet with unsteady averaging and a simple turbulent model*, Int. J. Heat Fluid Flow , Vol. 28, pp. 1125-1135

Minagawa Y., Obi S. (2004): *Development of turbulent impinging jet on a rotating disk,* Int. Journal of Heat and Fluid Flow, Vol. 25, pp. 759–766

Pellé J., Harmand S., (2007): *Heat transfer measurements in an opened rotor–stator system air gap,* Exp. Therm. Fluid Sci., Vol. 31, pp. 165-180

Randriamampianina A., Bontoux P., Roux B., (1987): *Ecoulements induits par la force gravitigue dans une cavite cylindrique en rotation*, Int. J. Heat Mass. Transfer, Vol. 30, pp. 1275-1292

Schouveiler L., Le Gal P., Chauve M.P., (2001): *Instabilities of the flow between a rotating and a stationary disk,* J. Fluid Mech., Vol. 443, pp. 329-350

Tsubokura M., Kobayashi T., Taniguchi N., Jones W.P., 2003, *A numerical study on the eddy structures of impinging jets excited at the inlet*, Int. J. Heat Fluid Flow, Vol. 24, pp. 500-511

Tsubokura, M., Kobayashi T., Taniguchi, N., (1997): *Large eddy simulation of plane impinging jets*. In: 11th Symp. Turb. Shear Flows, Grenoble, France, 8–10 September

Tuliszka-Sznitko E., Zielinski A., (2008), *DNS/LES of Transitional Flow in Rotating Cavity,* International Journal of Transport Phenomena, Vol. 10, 3, pp. 223-234, USA

Tuliszka-Sznitko E., Zieliński A., Majchrowski W., (2009a): *LES and DNS of the non-isothermal transitional flow in rotating cavity,* Int. Journal Heat Fluid Flow, Vol. 30, 3, pp. 534-548

Tuliszka-Sznitko E., Zieliński A., Majchrowski W., (2009b): *LES of the transitional flow in rotor/stator cavity,* Archives of Mech., Vol. 61, 2, pp. 93-118

Tuliszka-Sznitko E., Majchrowski W., Kiełczewski K., (2012): *Investigation of transitional and turbulent heat and momentum transport in rotating cavity,* Int. J. Heat and Fluid Flow, accepted, doi:10.1016/j.ijheatfluidflow.2012.02.002